A TWO-PHASE SIMPLIFIED COLLAPSE ANALYSIS OF RC BUILDINGS PHASE 1: SPRING NETWORK PHASE

Shanthanu RAJASEKHARAN[1], Muneyoshi NUMADA[2] and Kimiro MEGURO[3]

ABSTRACT: A simplified two-phase collapse simulation of RC structures is proposed. This paper discusses the nonlinear analysis of RC structures in the first phase, namely, the spring network phase. Application of spatially averaged (smeared crack) RC material models in the spring network is discussed. The material models are validated with a series of experiments conducted on RC panels. The results show the capability of the spring network to model the nonlinear behavior of RC.

Key Words: *Reinforced concrete, spring network, secant stiffness, smeared crack*

INTRODUCTION

Numerical simulation of the complete behavior of a building after the onset of an earthquake is important for understating its vulnerability to a seismic hazard and for providing necessary mitigation measures. There are various scientific methods to simulate the collapse of a building, however, they usually tend to be computationally extensive and complicated for practical vulnerability analysis of buildings. For ease of such analysis, the preferred characteristics are simple modelling, less computational expense, easy visualization and accuracy. The Distinct Element Method (DEM) (Cundall 1971) was initially introduced to model highly discontinuous and granular media, which comprised of domain discretization using rigid elements with springs at the point of contact. The approach of discretizing the structure into an assemblage of discrete elements and springs (Kawai 1977) (Shi 1985) (Tagel-Din 1998) is highly preferable due to its ability to capture element separation (crack initiation and propagation), with ease of modelling and lesser computational requirement as compared to continuum based analysis techniques such as the Finite Element Method (FEM).

In order to simulate total failure behavior from continuum to discrete medium, the Modified (or Extended) DEM (Meguro 1989) (Hakuno 1993) (Meguro 1994) was developed by introducing pore (or joint) springs that represent the continuous material media between elements (Figure 1). However, it has some limitations, namely, requirement of small time step, lack of a proper solid mechanics theory for spring stiffness derivation, and no consideration of the Poisson's ratio effect. By the usage of a spring network in the initial phase of simulation (pre-separation/collision) these limitations can be tackled.

First the overall simulation scheme, results from linear static analysis and the iterative secant stiffness formulation used are discussed. The smeared crack material models for concrete and steel used by the spring network are reviewed. The modifications that have to be made, in order to adopt the spatially averaged material models meant for non-linear finite element analysis into the spring network are discussed. The results are compared and verified based on experimental results obtained from a series of tests conducted on RC panels subjected to pure shear loading.

[1] Ph.D. candidate, Department of Civil Engineering.
[2] Assistant Professor, International Centre for Urban Safety Engineering (ICUS).
[3] Director/Professor, ICUS.

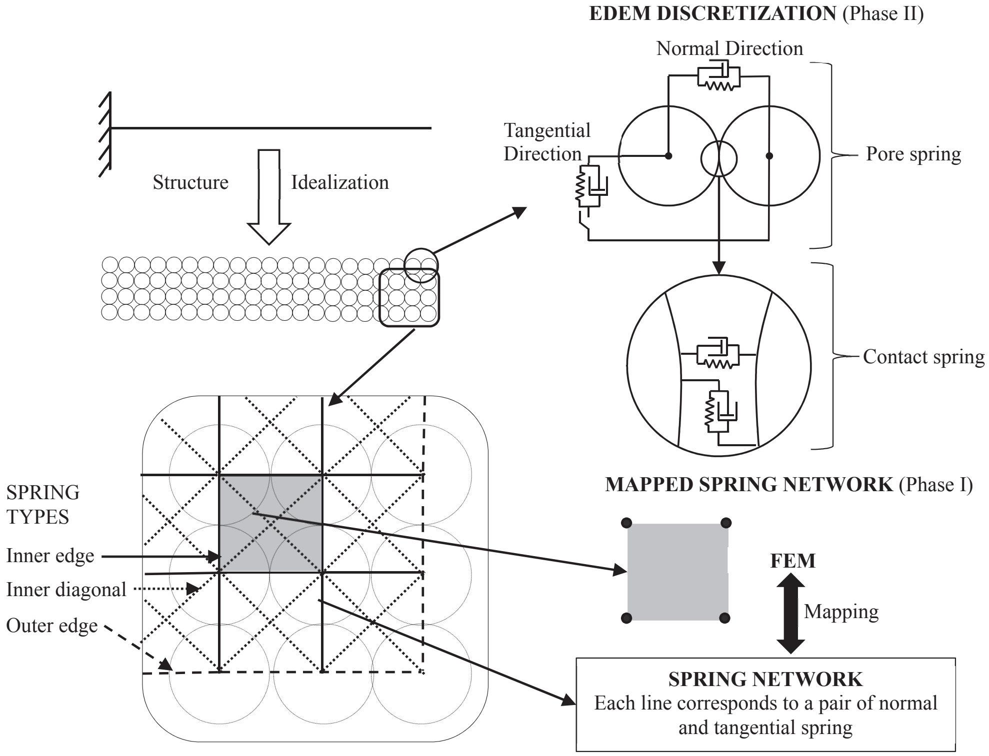

Figure 1. Domain discretization in EDEM and spring network

ANALYSIS PHASE

The analysis of the structure comprises of two phases: (i) Finite Element Mapped Spring Network Phase, (ii) Extended Distinct Element Method Phase. The overall behavior of the building from normal state to complete collapse state can be captured by these two phases (Figure 2).

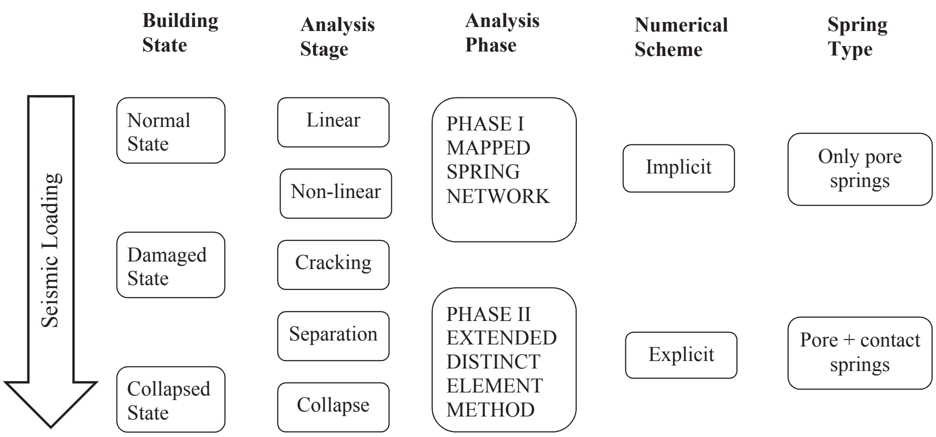

Figure 2. Domain discretization in EDEM and spring network

Finite Element Mapped Spring Network Phase

In this phase, the circular elements are connected through their centers only by the pore springs. The assembly of springs represents a spring network with lumped mass. The Finite Element (FE) mapping scheme for spring network representation of mechanics of solids (Gusev 2004), presented a rigorous method for spring stiffness derivation for any anisotropic infinite media. It essentially uses the property of translation invariance of the global stiffness matrix to equate the stiffness matrices obtained from finite element analysis and spring network assembly. Through this mapping procedure, the global stiffness matrix for the spring network is exactly the same as the global stiffness matrix obtained by finite element discretization.

The following advantages are obtained; (i) Due to global stiffness matrix assembly, an implicit time integration numerical scheme can be used, thereby increasing the critical time required for stable analysis, (ii) Accurate spring constants derivation, hence accuracy in the initial phase is high, (iii) Poisson's ratio is implicitly included, and (iv) Mass matrix is diagonal, which makes its inversion during dynamic analysis trivial.

For the current study, quadrilateral serendipity elements (two translational degrees of freedom at each node) are used for the derivation of the spring stiffness of the spring network. The elements were so chosen such that this spring network can be adopted during the EDEM phase. After the mapping it was found that were three kinds of springs based on their location (Table 1).

Table 1. Spring stiffness and local spring orientation for serendipity quadrilateral finite elements

<table>
<tr><th colspan="3">Spring type</th><th>Spring stiffness (Eigen Value)</th><th>Spring direction (Eigen direction)</th></tr>
<tr><td rowspan="4">Inner</td><td rowspan="2">Edge</td><td>normal</td><td>$\frac{E(3+\nu)}{6(1-\nu^2)}$</td><td rowspan="2">$\begin{pmatrix}1 & 0\\ 0 & 1\end{pmatrix}$
(Orthogonal)</td></tr>
<tr><td>tangent</td><td>$\frac{E.\nu}{3(-1+\nu^2)}$</td></tr>
<tr><td rowspan="2">Diagonal</td><td>normal</td><td>$\frac{E(9+\nu)}{24(1-\nu^2)}$</td><td rowspan="2">$\begin{pmatrix}1 & 0\\ 0 & 1\end{pmatrix}$
(Orthogonal)</td></tr>
<tr><td>tangent</td><td>$\frac{E(-3+5\nu)}{24(-1+\nu^2)}$</td></tr>
<tr><td colspan="2" rowspan="2">Outer edge</td><td>normal</td><td>$\frac{E\left(-3+\nu+6\sqrt{2}\sqrt{(\nu-\nu^2)}\right)}{24(-1+\nu^2)}$</td><td rowspan="2">$\begin{pmatrix}\frac{1+\nu-2\sqrt{2}\sqrt{(\nu-\nu^2)}}{-1+3\nu} & \frac{1+\nu+2\sqrt{2}\sqrt{(\nu-\nu^2)}}{-1+3\nu}\\ 1 & 1\end{pmatrix}$</td></tr>
<tr><td>tangent</td><td>$\frac{E\left(-3+\nu-6\sqrt{2}\sqrt{(\nu-\nu^2)}\right)}{24(-1+\nu^2)}$</td></tr>
</table>

Extended Distinct Element Method Phase

Once the deformations are considerable, the analysis switches to the conventional EDEM phase. The contact springs and the pore springs work in tandem and an explicit step-by-step time integration scheme is used for dynamic analysis. The advantage of this phase is that highly non-linear behavior, cracking, separation, collision and collapse can be captured in this phase efficiently. In discrete analysis, dynamic contact detection takes the majority of computation time (Williams 1999), however since the elements used in this analysis are simple circular/spherical elements, there is a large reduction in computation cost involved in contact detection during separation and collision.

LINEAR ELASTIC ANALYSIS

In order to check the accuracy of the assembled spring network, a simple linear analysis of bending of a cantilever beam was performed. The details of the cantilever are given in (Figure 3). With the increase in number of rows of elements, its influence on energy and error in deflection are observed. A normalized plot is shown below (Figure 4). The energy, size of element, time are normalized with their respective maximum values. The global stiffness matrix is exactly the same as the finite element stiffness matrix, hence it exhibits the same properties of that of the finite element system like energy convergence and error reduction with finer meshing. From these results, it was observed that the spring system leads to good results in the elastic range and the accuracy also depends on the kind of finite element used for derivation and also the meshing used. If this spring system is used in EDEM, it will essentially lead to a system which is accurate in its elastic phase.

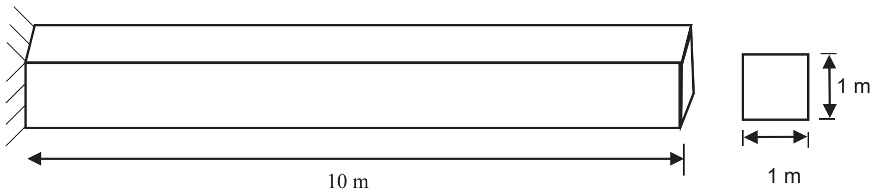

Young's Modulus, E = 2x10^9 Pa   Density = 8000 kg/m^3 Poisson's ratio, ν = 0.3

Figure 3. Properties of the cantilever used for linear analysis

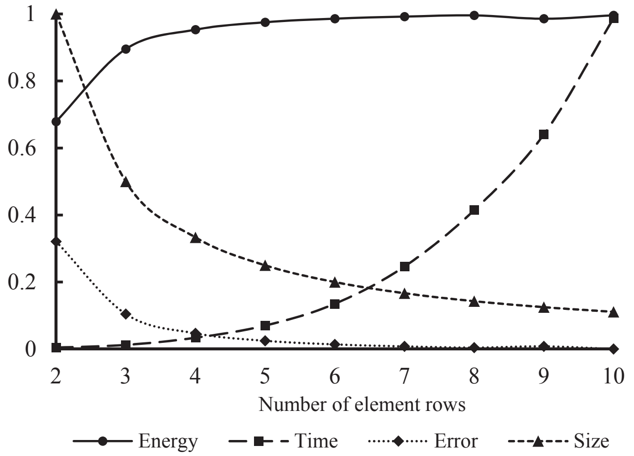

Figure 4. Linear static analysis: Variation of energy, displacement error with increase in elements

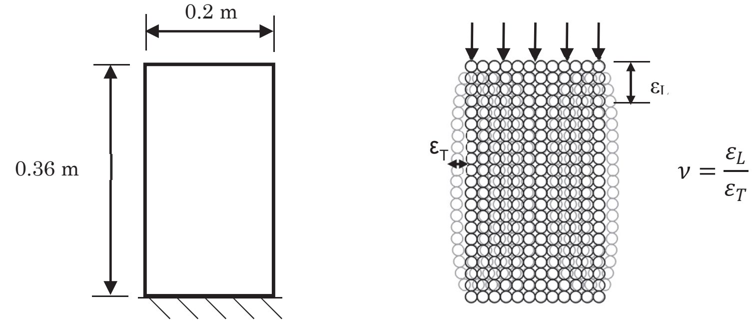

(a) Dimensions of the analyzed plate (b) EDEM discretization

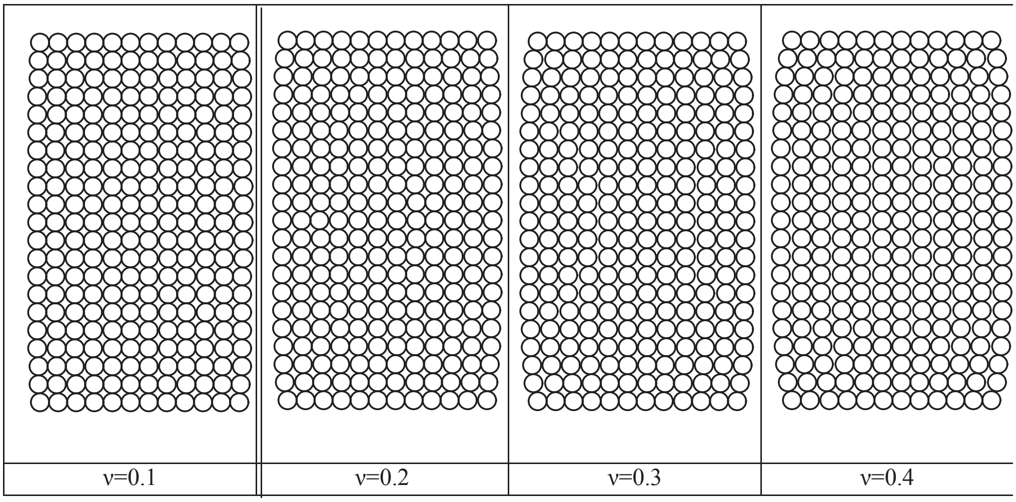

(c) Deformation profile with increasing Poisson's ratios (illustration scale factor is 100)

Figure 5. Poisson's ratio verification

Poisson's ratio

The Poisson's ratio is considered in the element constitutive relation while deriving the stiffness relations, during the finite element global stiffness matrix derivation. As the assembled stiffness matrices are the same, the spring constants implicitly model the Poisson's ratio effect. In order to demonstrate the capability of the spring network system to capture Poisson's ratio, a simple rectangular elastic plate of unit thickness, subjected to compression is considered (Figure 5). Constant strain is applied to the top row of elements and the elongation at the mid-level of the specimen is used to calculate the transverse strain for Poisson's ratio computation. While deriving the spring stiffness for the outer edge (boundary) springs, it was observed that the springs were not orthogonal to each other. However, a diagonal spring matrix can be obtained, if the springs are oriented along the eigen direction. Distinct diagonal spring stiffness for the boundary springs along the eigen direction can be obtained when the Poisson's ratio (ν) varies between $0.25 - \frac{5\sqrt{2}}{32} < \nu < 0.25 - \frac{5\sqrt{2}}{32}$ (~ 0.03 < ν < 0.47). As most conventional construction materials like steel and concrete lie within this range of Poisson's ratio, it can be assumed that distinct eigen values are always obtained while deriving the spring stiffness. When comparing the calculated and analytical Poisson's ratios (Figure 6), it can be seen the calculated values are very close to analytical values.

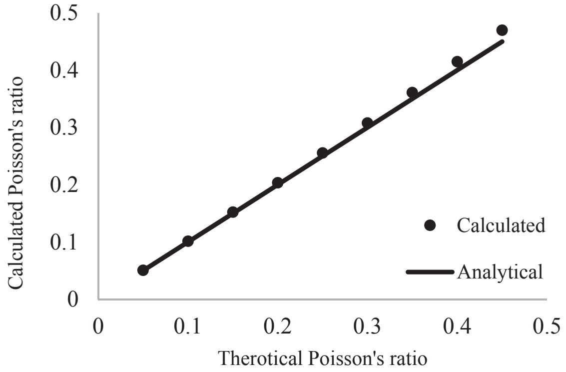

Figure 6. Comparison between calculated and analytical Poisson's ratios

ITERATIVE SECANT STIFFNESS FORMULATION

An iterative secant stiffness based formulation is used for computation, as it is numerically stable while handling complex material models (Vecchio 1989) and post peak response of structures. At every iterative step, secant modulus value of the total stress-strain relationship of the springs are updated till convergence. The flow of the program can be found below (Figure 7). It was observed that good convergence was obtained in around 20 iterations. One of the advantages of this method is that good accuracy can be obtained even with the use of relative simple finite elements.

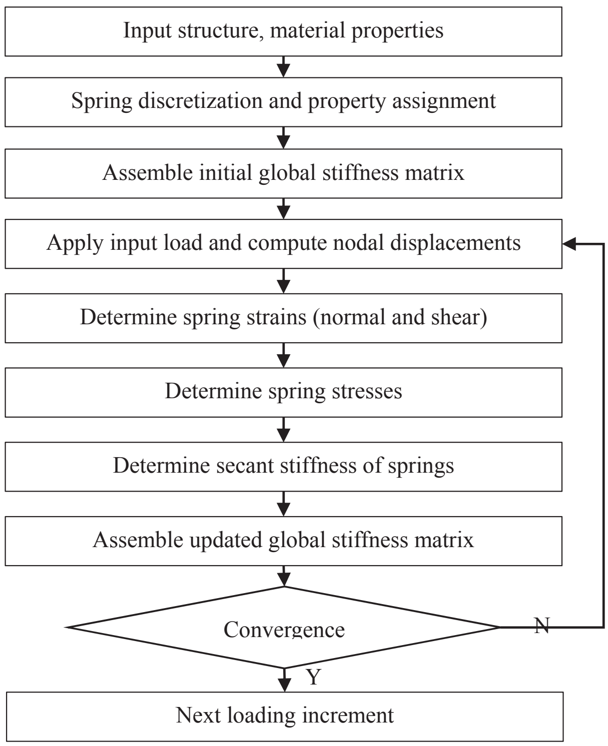

Figure 7. Flow chart of the analysis procedure

REINFORCED CONCRETE MATERIAL MODELS

A smeared crack approach for RC, consisting of spatially averaged constitutive models for concrete and reinforcing steel (Maekawa 2003), is adopted for the springs. Finite element analysis with these material models have shown to model accurately the nonlinear response of RC. The spring network model is analogous to the fixed smeared crack approach with the active crack assumed to be propagating along the direction of the springs. The current study involves the implementation of these models in a spring network system. Few modifications are made to the original models, including a Mohr-Coulomb failure criteria for the shear springs.

Compression model

There is a reduction of compressive strength along the direction of the crack and it is dependent on the lateral tensile strain. The cracking of springs is initiated when the tensile springs reach the maximum tensile stress. Once a spring cracks, the compressive strength of all the springs connected to the nodes of the cracked spring are reduced based on their lateral strain (Figure 8). This can be visualized as a zone created around the cracked spring with reduced compressive material models.

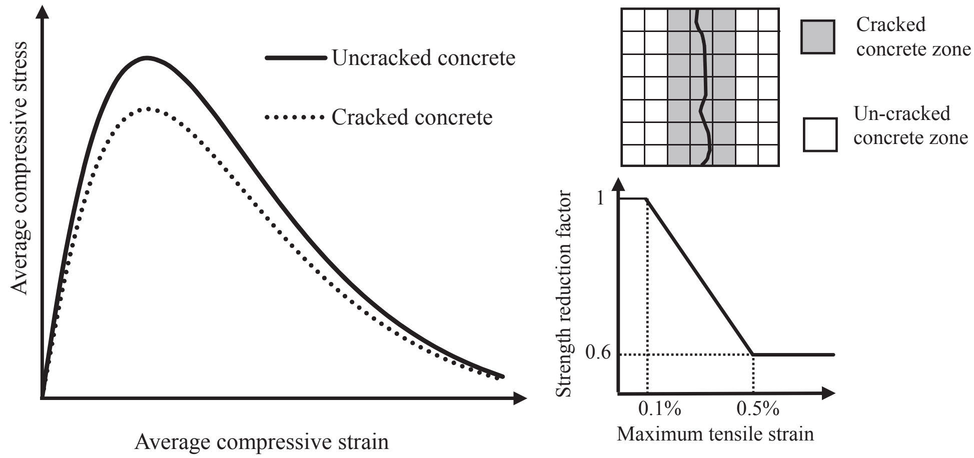

Figure 8. Compression model and reduced strength in cracked concrete zone

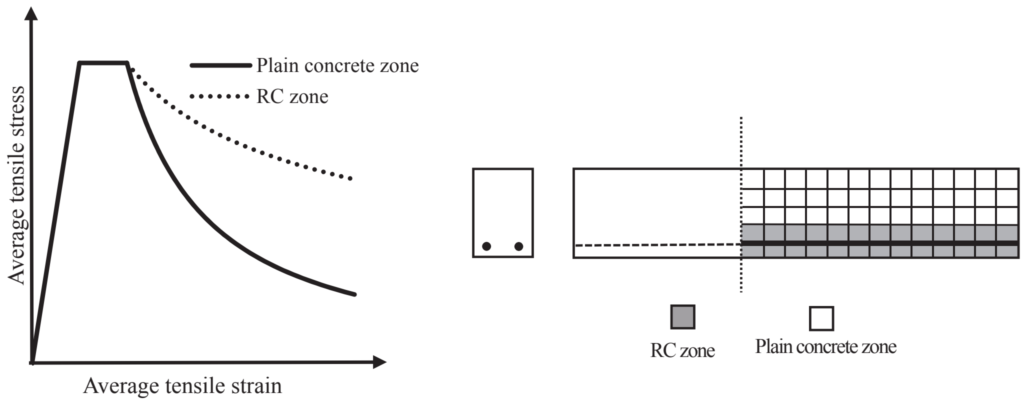

Figure 9. Tension model and definition of RC zone

Tension model
The concrete present near the reinforcing bars exhibit tension stiffening. During the discretization of the domain by the spring network, the springs are categorized based on the location with respect to the reinforcing bars. The springs connected to the nodes with reinforcing bars exhibit tension stiffening effect and these springs are assumed to be in the *RC zone* while the other springs are in the *Plain concrete zone* (Figure 9). The softening tension curve of the springs in the RC zone is less steep compared to the spring in the plain concrete zone in order to model the tension stiffening effect.

Shear model
In the case of FEM analysis, stress transformation is possible, therefore an explicit shear model and shear failure criteria is not required. In the case of spring network, stress transformation is not straightforward, hence a linear shear model is assumed up till a shear failure which is governed by the Mohr-Coulomb failure model (Figure 10). Post failure, a softening relationship exactly similar to the tension model is assumed. The Mohr-Coulomb parameters which were previously used for discrete RC analysis is used.

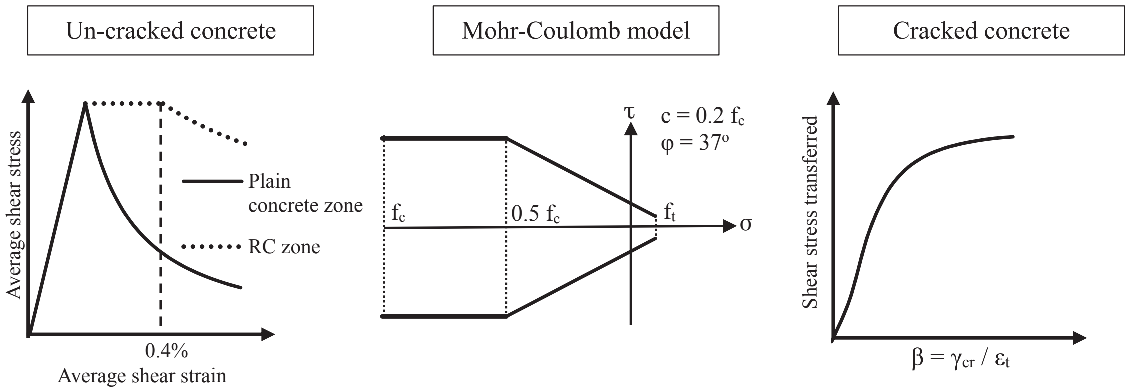

Figure 10. Shear models and failure criteria

Reinforcing steel model
An averaged steel stress-strain model is used instead of bare steel model in order to model the effects of concrete on the overall behavior of reinforcing steel (Figure 11).

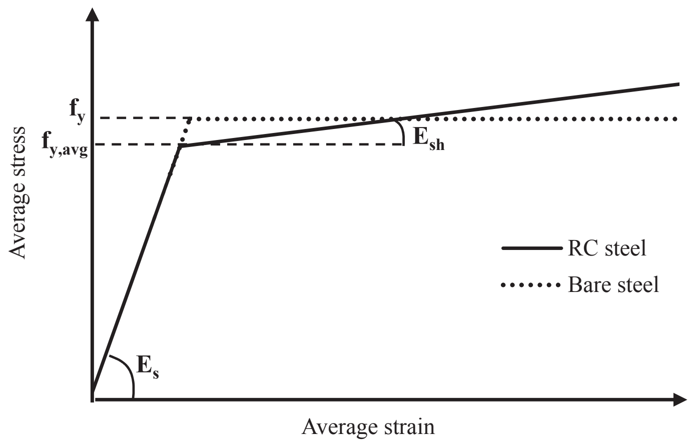

Figure 11. Averaged reinforcing steel model

EXPERIMENTAL VALIDATION

The PV series of experiments on RC panels (Collins 1982), are modeled to check the material models under monotonic loading conditions. The series of experiments consists of tests conducted on 30 RC panels (890mm x 890mm x 70mm) with varying loading conditions, reinforcement ratios and failure patterns (Table 2). In order to model the experiments, a spring network as shown below is used (Figure 12). The constant shear stress is applied through forces applied at the boundary nodes. For the current study, 9 panels subjected to pure shear loading.

Table 2. Properties of the RC panels used for analysis

Panel	Load ratio	Lon. Steel		Transverse Steel		Concrete		f_t
	(τ_{xy}:σ_x:σ_y)	ρ_x (%)	f_y	ρ_y (%)	f_y	ε_c	f_c	
PV3	1:0:0	0.0048	662	0.0048	662	0.0023	26.6	1.7
PV4	1:0:0	0.0106	242	0.0106	242	0.0025	26.6	1.9
PV6	1:0:0	0.0179	266	0.0179	266	0.0025	29.8	2.2
PV10	1:0:0	0.0179	276	0.01	276	0.0027	14.5	1.3
PV12	1:0:0	0.0179	469	0.0045	269	0.0025	16	1.6
PV19	1:0:0	0.0179	458	0.0071	299	0.0022	19	1.9
PV20	1:0:0	0.0179	460	0.0089	297	0.0018	19.6	2.0
PV21	1:0:0	0.0179	458	0.0130	302	0.0018	19.5	2.2
PV22	1:0:0	0.0179	458	0.0152	420	0.0020	19.6	2.3

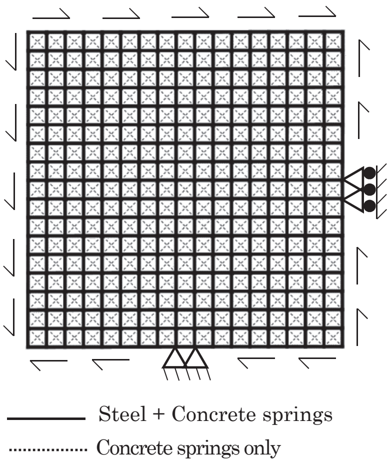

Figure 12. Spring network model of the experimental setup

RESULTS AND DISCUSSION

The results obtained from the analysis are given below (Figure 13). In the cases, where there was isotropic arrangement of steel and when steel yielding dominated the failure mode e.g. PV 3/PV 4, good correlation were observed with the experimental data. In two cases, PV 22 and PV 10 where the spring network became unstable due to excessive springs failing in shear, the analysis stopped before the specimen could reach its shear capacity. When the reinforcing ratio was not isotropic (PV 12, PV 19, PV 20, PV 21), it means there is shear slipping between the cracks, hence it can be used to check the shear contact models. In these cases too there was good co-relation between experimental and analysis data.

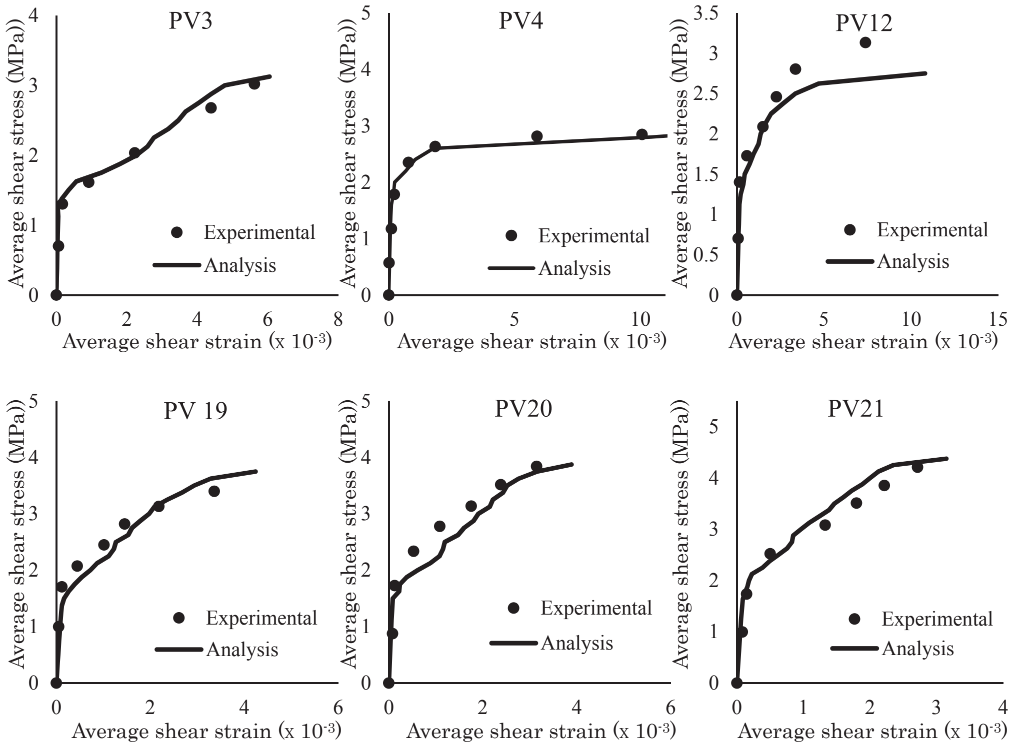

Figure 13. Comparison of experimental and analytical results for specimens under pure shear

CONCLUSION

A two phase analysis scheme was discussed. The accuracy of the spring network to model the linear static behavior of structure was discussed. The finite element mapped spring network essentially leads to a stiffness matrix exactly similar to the mapped finite element network. Hence the spring shows preferable properties such as more accurate results, convergence and implicit Poisson's ratio effect modeling.

The modifications required in order to use spatially averaged smeared crack models into a finite element mapped spring network was discussed. The results obtained from the simulations show the capability of the spring network to model the nonlinear behavior of RC panels under various monotonic loading conditions.

However, the results are sensitive to the input parameters, such as concrete tensile strength, shear strength (Mohr-Coulomb parameters), etc. A parametric study is needed to be performed in order to check the sensitivity of the results to the variations of these parameters. The study has to be extended to implement concrete models under cyclic loading conditions and further to dynamic cyclic loading conditions.

REFERENCES

Collins, M. P. and Vecchio, F. (1982). *The Response of Reinforced Concrete to In- Plane Shear and Normal Stresses,* University of Toronto, Canada.

Meguro, K. and Hakuno, M. (1989) "Fracture Analyses of Concrete Structures by the Modified Distinct Element Method." *Structural Engineering/Earthquake Engineering*, Vol.6 No.2, Japan Society of Civil Engineers (*Proceedings of JSCE No. 410*) 283s-294s.

Cundall, P. A. (1971). “A Computer Model For Simulating Progressive, Large Scale Movement in Blocky Rock System.” *Proc., Symposium of International Society of Rock Mechanics*, Nancy, France, Proc. 2, 129-136.
Gusev, A. (2004). “Finite Element Mapping for Spring Network Representations of the Mechanics of Solids.” *Physical Review Letters*, 93(3), 034302.
Hakuno, M., and Meguro, K. (1993). “Simulation of concrete-frame collapse due to dynamic loading.” *Journal of Engineering Mechanics*, 119(9), 1709–1723.
Kawai, T. (1977). “A new discrete model for analysis of solid mechanics problem.” *Journal of Seisan Kenkyu*, Inst. Ind. Sci. University Tokyo. 29, 208-210.
Maekawa, K., Pimanmas, A. and Okamura, H. (2003). *Nonlinear Mechanics of Reinforced Concrete*, London: Spon Press.
Meguro, K. and Hakuno, M. (1994). “Application of the extended distinct element method for collapse simulation of a double-deck bridge.” *Structural Engineering/Earthquake Eng*., Vol.10 No.4, Japan Society of Civil Engineers (*Journal of Structural Mechanics/ Earthquake Engineering* No. 483) 175s-185s.
Shi, G. and Goodman, R. E. (1985). “Two dimensional discontinuous deformation analysis.” *International Journal on Numerical and Analytical Methods in Geomechanics*, 9, 541-556.
Tagel-Din H. (1998). “*A New Efficient Method for Nonlinear, Large Deformation and Collapse Analysis of Structures.*” Ph. D. thesis, Civil Eng. Dept., The University of Tokyo.
Vecchio, F. J. (1989). “Nonlinear finite element analysis of reinforced concrete membranes.” *American Concrete Institute Structural Journal*, 86(1), pp. 26 – 35.
Williams, J. and O’Connor, R. (1999). “Discrete element simulation and the contact problem.” *Archives of Computational Methods in Engineering*, Vol. 6, 279–304